Mon. Not. R. Astron. Soc. **348,** 1197–1207 (2004) doi:10.1111/j.1365-2966.2004.07491.x

The distribution of atomic gas and dust in nearby galaxies – II. Further matched-resolution Very Large Array H I and SCUBA 850-μm images

H. C. Thomas,[1★] L. Dunne,[2] D. A. Green,[1†] M. S. Clemens,[3] P. Alexander[1] and S. Eales[2]

[1]*Mullard Radio Astronomy Observatory, Cavendish Laboratory, Madingley Road, Cambridge CB3 0HE*
[2]*Department of Physics and Astronomy, University of Wales Cardiff, PO Box 913, Cardiff CF2 3YB*
[3]*Dipartimento di Astronomia, Universita degli Studi di Padova, Vicolo dell'Osservatorio, 2, 35122 Padova, Italy*

Accepted 2003 November 16. Received 2003 November 10; in original form 2003 October 3

ABSTRACT

We present Very Large Array (VLA) C-array 21-cm H I images of galaxies from the SCUBA Local Universe Galaxy Survey which have been observed at 850 μm with the James Clerk Maxwell Telescope. Matched-resolution (∼ 25 arcsec) H I images of 17 galaxies are presented and compared with 850-μm images. H I or 850-μm images of an additional six galaxies which were detected at only one wavelength are presented. Additionally, lower resolution H I observations of nine galaxies are presented. The observations of these galaxies, along with results previously presented, do not show any obvious trends in the H I/dust or H_2/dust mass ratios with morphological type.

Key words: galaxies: abundances – galaxies: ISM – galaxies: structure – radio lines: galaxies.

Downloaded from http://mnras.oxfordjournals.org/ at Acquisitions on February 20, 2014

1 INTRODUCTION

The Submillimetre Common-User Bolometer Array (SCUBA) Local Universe Galaxy Survey (SLUGS, see Dunne et al. 2000; Dunne & Eales 2001; Thomas et al. 2002) is a major survey of dust emission in 104 nearby galaxies, as observed with the SCUBA instrument on the James Clerk Maxwell Telescope (JCMT). Although it provides important data on the dust emission from a much larger number of galaxies than has previously been available, comparison with observations of other components of the ISM of the galaxies is also valuable. This is the second of a series of three papers in which we investigate the relationship of the dust emission to the neutral hydrogen (H I) emission. In (Thomas et al. (2002, hereafter Paper I), matched-resolution H I images of 20 SLUGS galaxies from Very Large Array (VLA) C-array observations were presented and compared with the 850-μm images. Here similar data for a further 24 SLUGS galaxies are presented, together with lower resolution VLA D-array H I observations of some larger (>2.5 arcmin) galaxies from the SLUGS sample. The observations and the data reduction are briefly discussed in Section 2, and the results presented in Section 3. The overall properties of the dust and H I in the galaxies presented here and in Paper I are discussed in Section 4. Analysis and discussion of their radial distributions are the subjects of a future paper (Thomas et al. 2004, Paper III). The lower resolution D-array observations are discussed in the Appendix.

★Present address: 12 Middlehurst Ave, Weaverham, Northwich CW8 3BW.
†E-mail: dag@mrao.cam.ac.uk

2 VLA OBSERVATIONS AND DATA REDUCTION

Galaxies were selected from the SLUGS sample with angular sizes (D_{25}) less than 3 arcmin. From this we chose 24 galaxies to observe at 21 cm with the VLA in C-array in 2001 July. Table 1 lists the sample. These 24 galaxies consist of 13 *IRAS* selected galaxies, plus 11 optically selected (see Dunne et al. 2000; Dunne 2000, and Table 1), whereas the galaxies in Paper I consisted solely of *IRAS* selected galaxies. The observations were made, and the data reduced, in a similar way to that described in detail in Paper I (see Section 3.1). In addition, a small sample of 13 SLUGS galaxies larger than 2.5 arcmin in size were observed in 1999 April with the VLA in D-array. These observations are of lower resolution (typically 50 arcsec) than the SCUBA 850-μm observations, and therefore do not provide matched-resolution H I images. However, the D-array observations are more sensitive to emissions on larger scales, and are useful to determine the overall extent of H I in larger galaxies. Three of the galaxies (NGC 958, 5020 and 5962) observed in D-array were also observed in C-array. Of the 10 other galaxies observed in D-array, nine were detected, and the results for these galaxies are presented in the Appendix.

3 RESULTS

Of the 24 galaxies observed in H I, emissions from 17 were clearly detected and one was barely detected (NGC 7047, see discussion below). Five galaxies were not detected in H I (IC 5090, IC 1368 and NGC 6120, detected at 850 μm; IC 1211 and UGC 10500, not detected at 850 μm), and one (Arp 220) was detected in absorption.

© 2004 RAS

Table 1. General properties of the sample.

Name (1)	RA (B1950) (2)	Dec. (B1950) (3)	Type (4)	Nuclear type (5)	Distance $75/H_0$ (Mpc) (6)	$\log_{10}(L_{FIR})$ ($L_\odot$) (7)	Sample
UGC 148	00 13 16.3	+15 48 43	S?	–	57.1	10.34	O
NGC 99	00 21 23.8	+15 29 37	Scd	–	70.1	10.14	O
NGC 958	02 28 11.0	−03 09 44	Sc	–	79.9	10.97	I
NGC 992	02 34 35.6	+20 53 04	S?	–	54.2	10.78	I
NGC 1222	03 06 25.6	−03 08 43	E/S0	–	33.6	10.36	I
UGC 2982	04 09 43.0	+05 25 12	Sm	H II	67.0	10.99	I
NGC 4433	12 25 03.8	−08 00 09	Sab	–	41.9	10.64	I
NGC 4793	12 52 15.6	+29 12 34	Sc	–	36.7	10.54	I
NGC 5020	13 10 10.7	+12 51 53	Sbc	–	44.8	10.38	I
NGC 5937	15 28 09.9	−02 39 33	Sb	–	33.9	10.83	I
NGC 5953/4	15 32 13.2	+15 21 37	Sa/Scd	Sy2/Sy2	22.3	10.21	I
Arp 220	15 32 46.8	+23 40 08	S?	H II; Sy2	75.8	11.94	I
NGC 5962	15 34 14.0	+16 46 21	Sc	H II	29.6	10.19	I
UGC 10200	16 04 03.7	+41 28 43	S?	H II	25.7	–	O
IC 1211	16 15 38.2	+53 07 40	E	–	75.4	–	O
NGC 6120	16 18 01.2	+37 53 36	S?	H II	121.9	11.13	O
UGC 10500	16 38 05.1	+57 49 17	S0/a	–	71.9	–	O
IC 5090	21 08 55.0	−02 14 17	Sa	–	120.0	11.14	O
IC 1368	21 11 40.4	+01 58 13	Sa	Sy 2	52.4	10.34	O
NGC 7047	21 13 53.0	−01 02 08	Sb	–	75.9	10.05	O
NGC 7081	21 28 52.1	+02 16 12	Sb	–	44.3	9.93	O
NGC 7591	23 15 43.9	+06 18 45	Sbc	LINER	63.8	10.84	I
NGC 7722	23 36 09.3	+15 40 39	S0/a	–	50.6	10.05	O
UGC 12914/5	23 59 06.8	+23 12 55	Scd/Sc	LINER/LINER	63.0	10.70	I

Notes: (1) Galaxy name. (2) and (3) RA and Dec. (B1950). (4) Morphological type. (5) Spectral type. (6) Distance, from recession velocity. (7) For *IRAS*-selected SLUGS galaxies, far-infrared luminosity from Dunne et al. (2000) and Dunne (2000). (8) Sample, either 'I' for infrared or 'O' for optically selected.

The total H I flux density of each galaxy, or a limit, was determined from the integrated H I images. For galaxies not detected, $3\sigma_{\rm rms}$ upper limits on the amount of H I were estimated by assuming a typical velocity width of 350 km s^{-1}. These results are given in Table 2. As found in Paper I, the VLA observations recover typically ~70 per cent of the total H I flux found in single-dish H I observations in the literature. The missing flux is due to the limited sensitivity of the C-array observations to extended emission on scales greater than about 3 arcmin, i.e. on scales larger than those measured by the SCUBA 850-μm observations.

The matched-resolution (25 arcsec) H I and 850-μm images of 17 of the selected SLUGS galaxies detected in both H I and at 850 μm are shown in Fig. 1, where the field-of-view has been chosen to match the extent of the 850-μm data. In four of these galaxies (NGC 4793, 5020, 5962 and 7591), the extent of the H I emission is much larger than that of the SCUBA field of view – the H I images from these galaxies over wider fields of view are shown in Fig. 2. A wide-field view of the H I detected in UGC 10200, which was not detected at 850 μm, is shown in Fig. 3. SCUBA 850-μm images of the galaxies not detected (NGC 6120, NGC 5090 and IC 1368), or only weakly detected in H I (NGC 7047) are shown in Fig. 4.

3.1 Notes on some individual sources

3.1.1 NGC 958

At 850 μm the small companion galaxy to the south-east was also detected, although the emission does not appear to be well correlated with the H I. The H I distribution is somewhat irregular beyond the edge of the optical disc of NGC 958 and extends towards the south. The lower-resolution, larger field D-array H I image of NGC 958, shown in Fig. 5, reveals a faint bridge of emissions stretching to a small companion galaxy to the north-west.

3.1.2 NGC 992

The H I distribution of NGC 992 shows diffuse emissions extending to Mrk 369, a small elliptical 2.6 arcmin to the north-west. The mean recession velocity of Mrk 369, as determined from the H I data, is 4050 km s^{-1} which is consistent with the optical velocity of 4045 km s^{-1} (Huchra, Vogeley & Geller 1999). There is likely to be diffuse, extended H I associated with the pair which was not detected by this snap-shot observation, as single-dish observations detect more H I flux.

3.1.3 NGC 5937

The 850-μm emission is concentrated towards the optical centre of this galaxy, whereas the H I associated with NGC 5937 is significantly offset from its centre. NGC 5937 has no nearby companions.

3.1.4 Arp 220

This is the most luminous infrared galaxy in the *IRAS* bright galaxy sample, the brightest at 850 μm. It is at a distance of 72.5 Mpc, and has a far-infrared luminosity of ~10^{12} $L_\odot$. It is the closest, and hence most well studied, of all ultraluminous infrared galaxies (e.g. Soifer et al. 1999; Anantharamaiah et al. 2000; Wiedner

Downloaded from http://mnras.oxfordjournals.org/ at Acquisitions on February 20, 2014

Table 2. Gas and dust masses.

Name	$S_{\rm H\,I}$ (Jy km s^{-1})	$\log_{10}(M_{\rm H\,I})$ (M$_\odot$)	$\log_{10}(M_{\rm d})$ (M$_\odot$)	$\log_{10}(M_{\rm H_2})$ (M$_\odot$)	Refs	$M_{\rm H_2}/M_{\rm H\,I}$	$(M_{\rm H2}+M_{\rm H\,I})/M_{\rm d}$
(1)	(2)	(3)	(4)	(5)	(6)	(7)	(8)
UGC 148	6.1 ± 0.5	9.67	7.76	–		–	–
NGC 99	12.6 ± 1.3	10.16	7.77	–		–	–
NGC 958	26.0 ± 2.7	10.59	8.34	10.21	a,b	0.42	252
NGC 992	9.0 ± 1.1	9.79	7.74	9.77	a,c,d,e,f	0.95	219
NGC 1222	6.9 ± 0.8	9.26	7.07	–		–	–
UGC 2982	5.8 ± 0.6	9.79	7.99	10.06	c,g	1.86	180
NGC 4433	12.4 ± 1.3	9.71	7.70	9.62	g	0.81	186
NGC 4793	32.5 ± 3.6	10.01	7.64	9.49	a,g,h	0.30	305
NGC 5020	23.0 ± 2.4	10.04	7.73	9.30	i	0.18	241
NGC 5937	2.2 ± 0.5	8.78	7.57	–		–	–
NGC 5953/4	6.1 ± 0.6	8.86	7.30	8.99	j,k	1.35	85
Arp 220	A	<10.64	8.79	10.44	a,b,g	>0.63	–
NGC 5962	18.4 ± 1.9	9.58	7.56	9.67	g,k	1.23	233
UGC 10200	8.5 ± 1.0	9.12	<6.17	–		–	–
IC 1211	<0.7	<8.97	<7.13	–		–	–
NGC 6120	<1.7	<9.78	8.09	–		–	–
UGC 10500	<2.1	<9.41	–	–		–	–
IC 5090	<1.9	<9.81	8.36	–		–	–
IC 1368	<2.0	<9.11	7.17	–		–	–
NGC 7047	<1.8	<9.39	7.60	–		–	–
NGC 7081	7.3 ± 0.8	9.53	7.16	–		–	–
NGC 7591	22.5 ± 2.4	10.33	7.85	10.23	f	0.79	541
NGC 7722	1.4 ± 0.3	8.93	7.52	9.62	l	4.90	152
UGC 12914/5	9.6 ± 1.0	9.95	8.00	10.41	m	2.88	346

Notes: (1) Galaxy name. (2) VLA H I flux and error. 'A' indicates the galaxy was only observed in absorption. (3) The H I gas mass, calculated from $2.36 \times 10^5\, D^2\, S_{\rm H\,I}$, where D is the distance to the source in Mpc. (4) Dust mass taken from Dunne et al. (2000). (5) Molecular gas mass, assuming a CO-to-H$_2$ conversion factor of $X = 2.8 \times 10^{20}$ H$_2$ cm^{-2} (Kenney & Young 1989). (6) References for the CO fluxes are: (a) Sanders, Scoville & Soifer (1991); (b) Maiolino et al. (1997); (c) Chini, Krügel & Lemke (1996); (d) Elfhag et al. (1996); (e) Sanders & Mirabel (1985); (f) Lavezzi & Dickey (1998); (g) Young et al. (1995); (h) Casoli et al. (1996); (i) Seaquist, private communication; (j) Sofue et al. (1993); (k) Tinney et al. (1990); (l) Wang et al. (1992); (m) Zhu et al. (1999). (7) Molecular gas to atomic gas mass ratio [calculated from columns (3) and (5)]. (8) Gas-to-dust mass ratio [calculated from columns (3) to (5)].

et al. 2002; McDowell et al. 2003). Arp 220 showed strong H I absorption.

3.1.5 *NGC 7047*

This galaxy was a weak detection at 850 µm. The H I line profile reveals only weak ($\sim 2\sigma$) emission around the systemic velocity of 5650 km s^{-1} when integrated over the galaxy. Theureau et al. (1998) recorded an H I flux of 0.9 Jy km s^{-1} which is consistent with the upper limit derived from these observations.

3.1.6 *NGC 7722*

Although the H I emission associated with NGC 722 is weak, it is aligned along the dust lane visible in the optical image. The dip in the H I approximately coincides with the peak in the 850-µm emission. Although there is a radio continuum source at the centre of the galaxy, it is too weak to explain the dip in the H I as the result of absorption. Wang, Kenney & Ishizuki (1992) observed NGC 7722 in CO ($J = 1 \rightarrow 0$, with a beam of 16 arcsec) and found a molecular gas mass of $\sim 10^9$ M$_\odot$. Although this observation was positioned at the radio centre (rather than at the H I dip), this galaxy is rich in molecular gas which may explain the lack of H I.

3.1.7 *UGC 12914/5*

The H I image of UGC 12914/5 (the 'Taffy' galaxies) is in good agreement with the C-array VLA image of Condon et al. (1993, their fig. 4). However, less H I flux (9.6 Jy km s^{-1} compared with 15.3 Jy km s^{-1}) is recovered from the present observations, due to the fact that Condon et al. performed a full synthesis (10 h) observation, and they were therefore more sensitive to emission on larger angular scales. Radio continuum observations by Condon et al. revealed that approximately half of the 1.4-GHz emission arises between the two galaxies. This excess emission gives UGC 12914/5 the lowest far-infrared/radio ratio of all the 258 galaxies in the *IRAS* bright galaxy survey. Condon et al. propose a bridge of cosmic rays, magnetic fields and H I gas have been stripped from the discs of the galaxies, after a head-on collision $\sim 2 \times 10^7$ yr ago. The 850-µm image shows tentative evidence for a bridge of 850-µm emission between these two galaxies, which approximately follows the peak H I contour.

4 DISCUSSION

4.1 Gas and dust morphology

As was seen in Paper I, it is rare for the 850-µm and H I peaks to coincide. In many cases the 850-µm peak is found at the location of a

Downloaded from http://mnras.oxfordjournals.org/ at Acquisitions on February 20, 2014

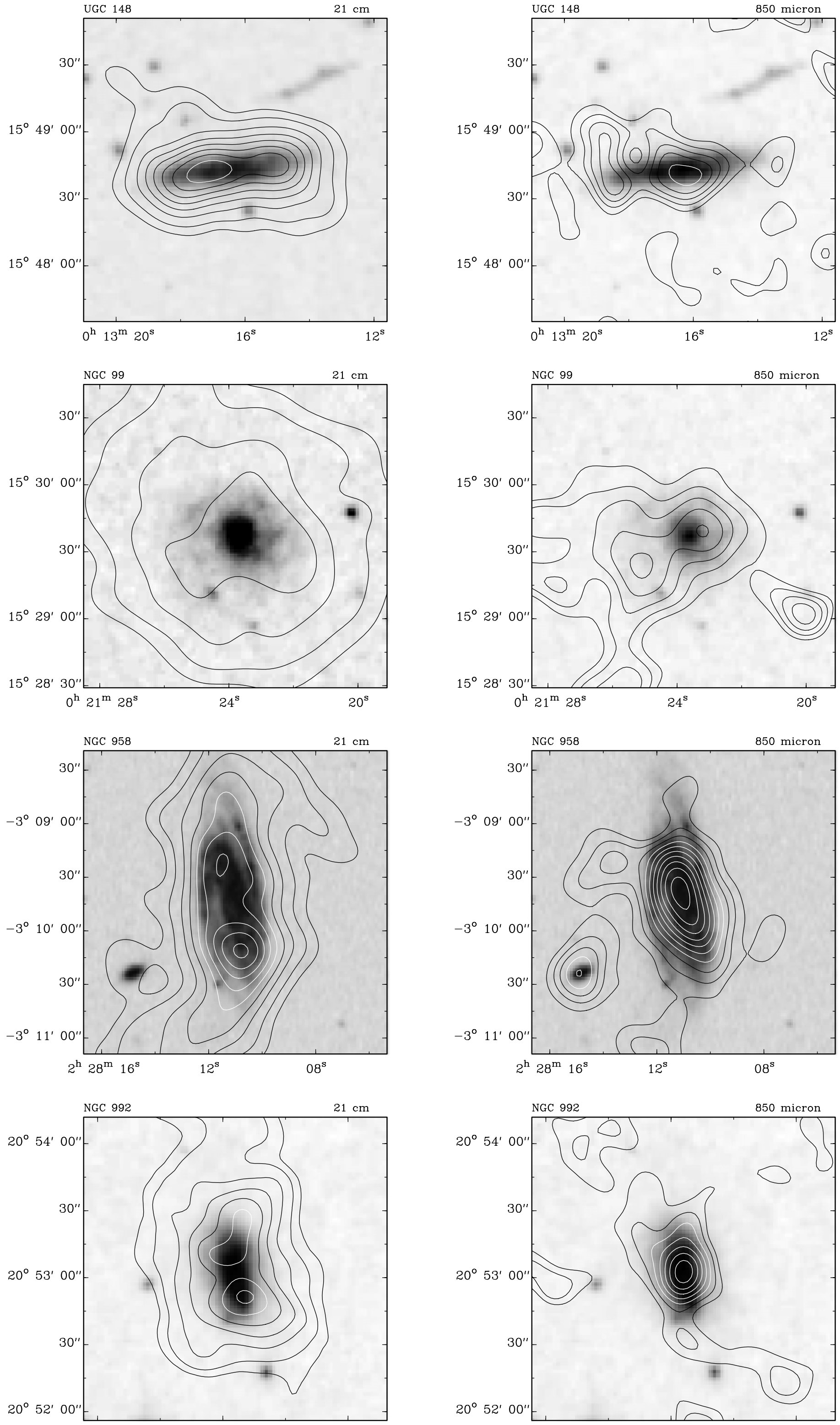

Figure 1. VLA C-array H I images, with continuum subtracted (left) and SCUBA 850-μm images (right) convolved to a resolution of 25 arcsec and overlaid on an optical (*R*-band) Digitized Sky Survey image. The contours for the H I images are ± (0.2, 0.5, 1.0, 1.5, 2.0 ...) × 10^{21} atom cm^{-2}, where negative contours are dashed, and positive contours solid. The contours for the 850-μm images are 10, 20, 30, 40... mJy $beam^{-1}$. All images are 2.3 arcmin in extent, which is the SCUBA field of view. (Larger field of view images of NGC 4793, 5020, 5962 and 7591 are shown in Fig. 2.)

Downloaded from http://mnras.oxfordjournals.org/ at Acquisitions on February 20, 2014

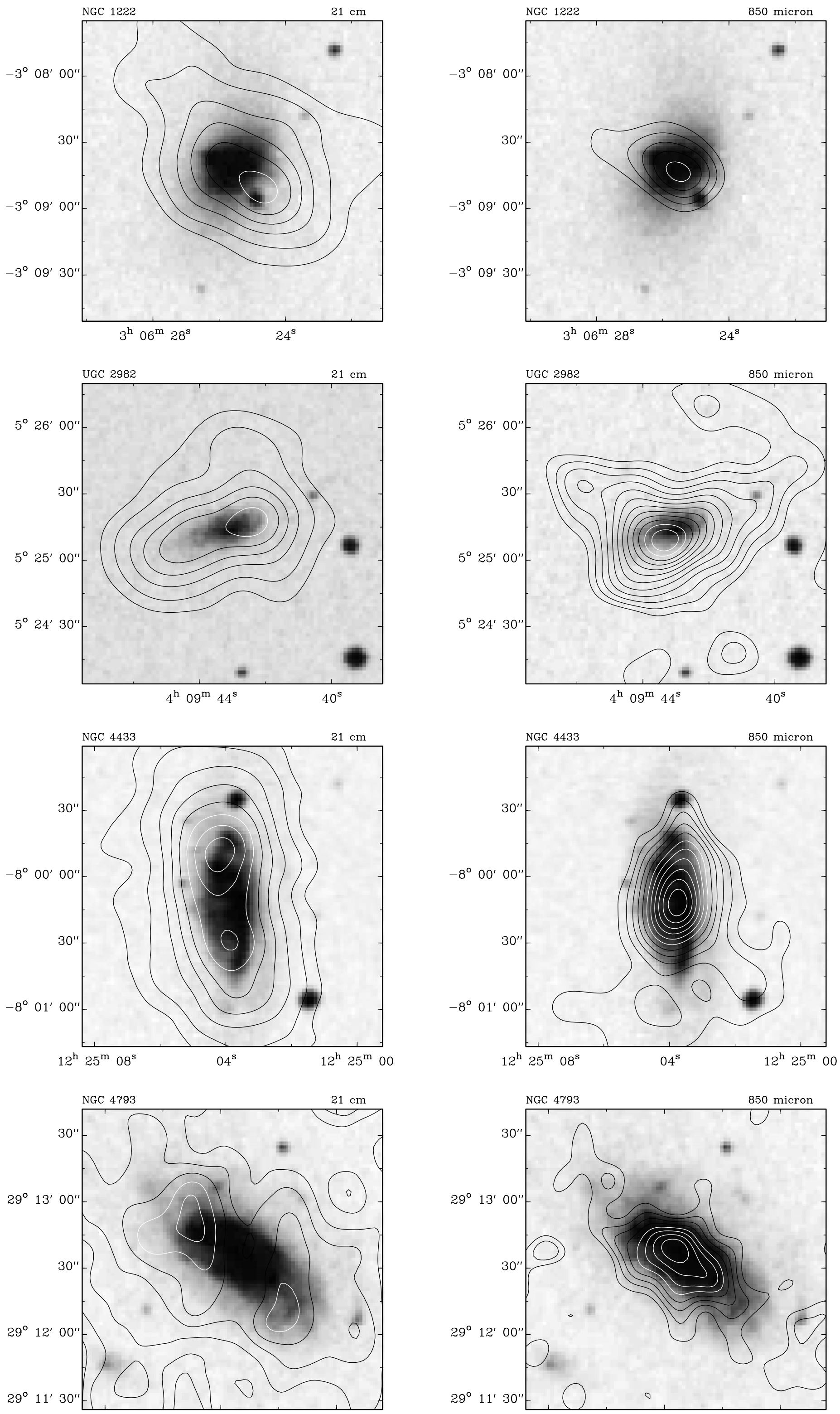

Figure 1 – *continued*

local H I minimum, often, but not always, at the centre of the galaxy. This anti-correlation has three possible explanations as follows.

(i) H I absorption against the radio continuum emission accompanying the 850-μm flux reduces the observed line flux.

(ii) The dust mass distribution is similar to the H I distribution but the dust temperature or emissivity rises sharply in the centre of the sources; due to either a starburst nucleus or active galactic nucleus.

(iii) Conversion of H I to H_2 is greater in dusty regions.

Downloaded from http://mnras.oxfordjournals.org/ at Acquisitions on February 20, 2014

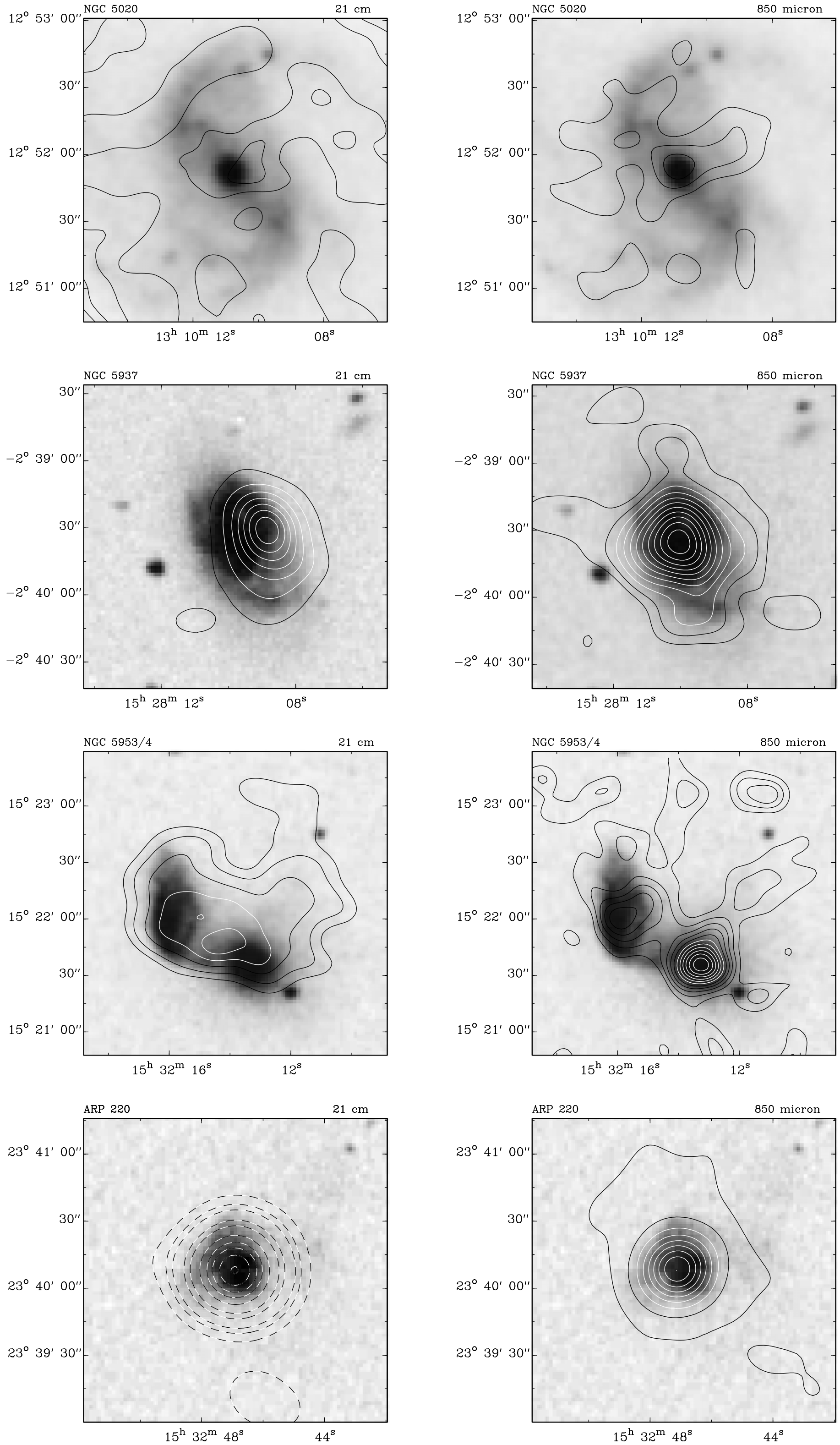

Figure 1 – *continued*

As discussed in Paper I, the brightness temperature of the continuum from the centre of galaxies, as observed at 1.4 GHz with a 20-arcsec beam, is large compared with the typical H I emission observed. Consequently even very small optical depths will produce significant absorption towards the centres of these galaxies compared with the H I emission. In addition, those galaxies that show a central H I minimum tend to have higher inclinations than those that do not, which favours the absorption hypothesis.

Downloaded from http://mnras.oxfordjournals.org/ at Acquisitions on February 20, 2014

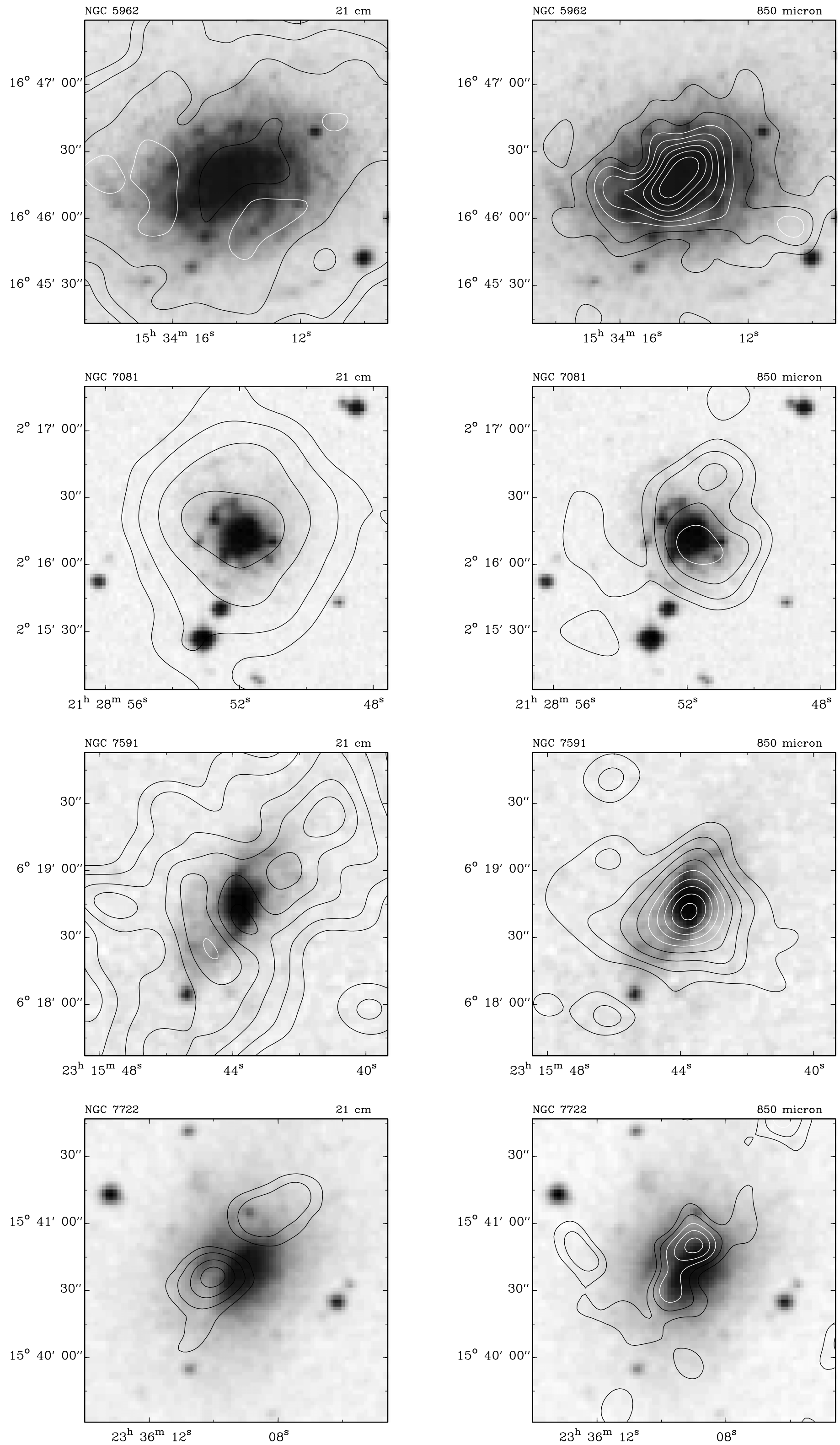

Figure 1 – *continued*

The second possibility requires spatially resolved data that trace the dust temperature, which we do not have. The 450-μm data from the SLUGS survey are generally not of sufficient quality to trace the radial temperature profile. However, even for an AGN-dominated source such as NGC 4418, Dunne & Eales (2001) find a dust temperature no higher than 60 K for the warm component. As the 850-μm flux is approximately proportional to temperature, it seems unlikely that the large rise in far-infrared emission towards the centre of these

Downloaded from http://mnras.oxfordjournals.org/ at Acquisitions on February 20, 2014

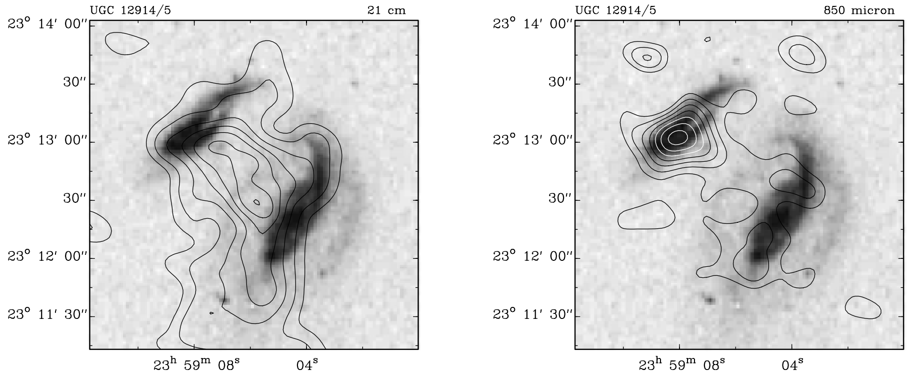

Figure 1 – *continued*

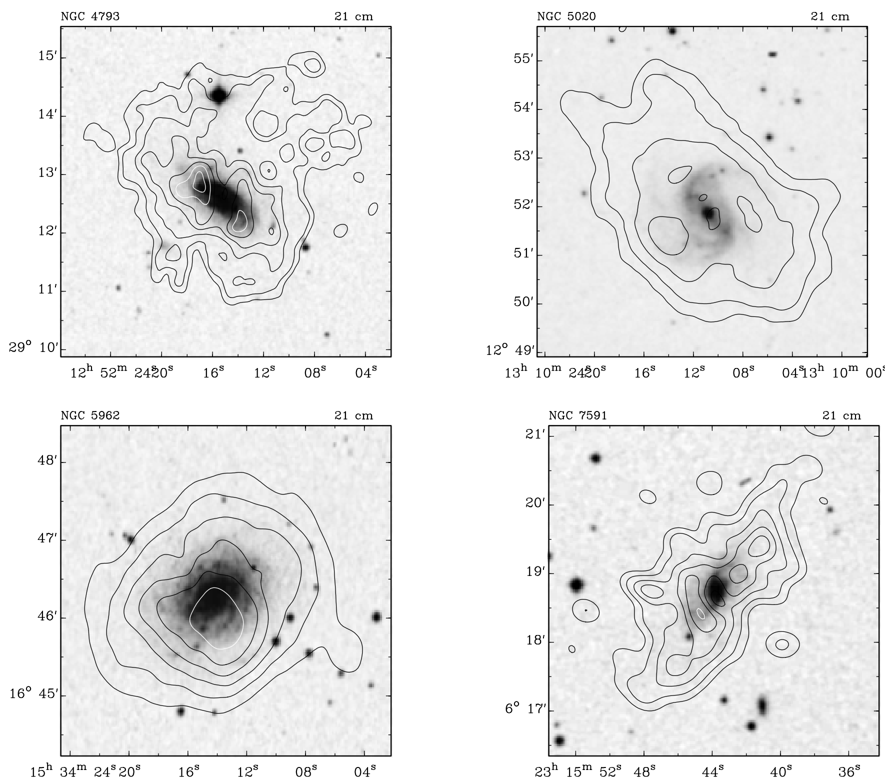

Figure 2. VLA C-array H I images of NGC 4793, 5020, 5962 and 7591, covering a wider field than shown in Fig. 1. The contours are ± (0.2, 0.5, 1.0, 1.5, 2.0 . . .) × 10^{21} atom cm^{-2}. The NGC 4793 and 7591 images are from C-array data alone, and have a resolution of 25 arcsec. The NGC 5020 and 5962 images are from combined C- and D-array data, and have a resolution of 40 arcsec.

sources could be due entirely to a temperature increase. It is unlikely that this can explain the frequent coincidence of H I minima with 850-μm maxima.

If H I had been processed to H_2 in the centre of these sources, as might be expected for a central starburst for example, we would expect to see a central concentration of molecular gas. CO observations of the objects are needed in order to test this possibility.

As H I absorption is almost certainly important for most of the sources in this sample the importance of this effect would need to be determined before considering the possibility of processing between atomic and molecular gas components.

4.2 Gas and dust masses

Combining the results from this paper with those presented in Paper I, a comparison of the overall H I, dust and H_2 masses of the *IRAS*

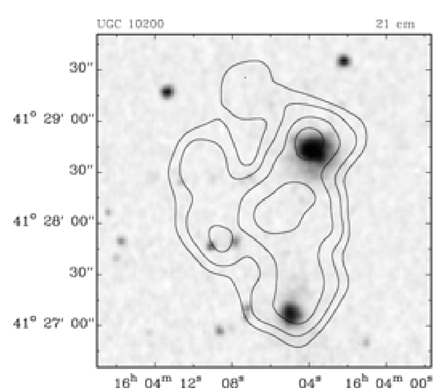

Figure 3. VLA C-array H I image of UCG 10200, which was not detected at 850 μm. The contours are ± (0.2, 0.5, 1.0, 1.5, 2.0 . . .) × 10^{21} atom cm^{-2}, and the resolution is 25 arcsec.

Downloaded from http://mnras.oxfordjournals.org/ at Acquisitions on February 20, 2014

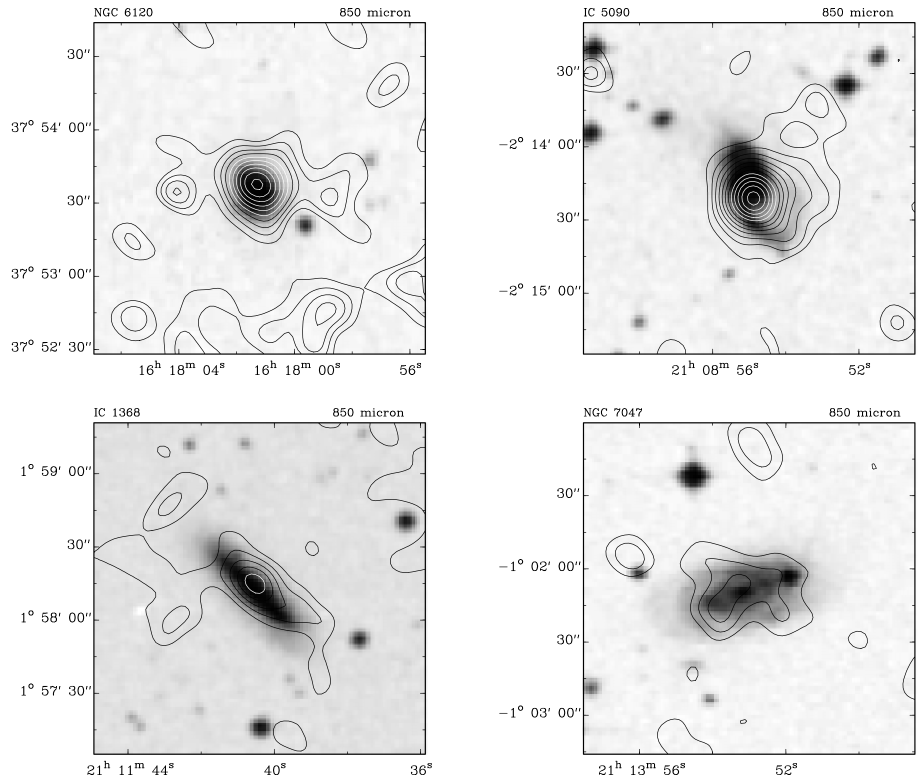

Figure 4. SCUBA 850-µm images of galaxies not detected, or only weakly detected, in H I. The data have been smoothed to a resolution of 20 arcsec. The contours are at 5, 10, 15, 20... mJy beam^{-1}.

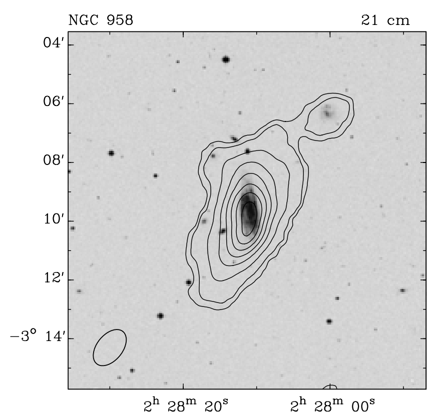

Figure 5. VLA H I image of NGC 958, from VLA D-array data. The contours are ± (0.5, 1, 3, 6, 9...) × 10^{20} atom cm^{-2}, and the resolution is 124 × 60 arcsec^2, as indicated by the ellipse in the bottom left corner.

bright sample galaxies can be made. Excluding galaxies in pairs, and those only detected in absorption, H I and dust masses are available for 20 galaxies, and the H I/dust mass ratio averaged over two bins by morphological type (Sa to Sbc, and Sc to Sd, each with 10 galaxies) are given in Table 3. For 14 of these galaxies H_2 masses are also available, and the H_2/dust, H I/H_2 and gas/dust (i.e. H I and H_2 to dust) mass ratios for these galaxies are also given in Table 3. From these results, none of the mass ratios shows any obvious dependence on morphological type.

5 CONCLUSIONS

We have presented further matched-resolution H I and 850-µm images of galaxies from the SLUGS sample. Most galaxies are from the *IRAS* bright sample in SLUGS, but some are from an optically selected sample. Although the 850-µm emission generally peaks near the centres of the galaxies, the H I images often show minima, which are probably due to absorption. For the *IRAS* selected galaxies, these observations, along with results previously presented, do not show any obvious trends in the H I/dust or H_2/dust mass ratios with morphological type.

ACKNOWLEDGMENTS

The National Radio Astronomy Observatory is a facility of the National Science Foundation operated under cooperative agreement by Associated Universities, Inc. The JCMT is operated by the Joint

Table 3. The mean properties of $M_{\rm H\,I}/M_{\rm d}$, $M_{\rm H_2}/M_{\rm d}$, $M_{\rm H\,I}/M_{\rm H_2}$ and $M_{\rm g}/M_{\rm d}$ as a function of morphological type.

Type	Number	$\left\langle \frac{M_{\rm H\,I}}{M_{\rm d}} \right\rangle$	Number with $M_{\rm H_2}$	$\left\langle \frac{M_{\rm H_2}}{M_{\rm d}} \right\rangle$	$\left\langle \frac{M_{\rm H\,I}}{M_{\rm H_2}} \right\rangle$	$\left\langle \frac{M_{\rm g}}{M_{\rm d}} \right\rangle$
Sa/Sab/Sb/Sbc	10	173 ± 45	7	270 ± 74	2.14 ± 0.92	474 ± 118
Sc/Scd/Sd	10	197 ± 35	7	206 ± 101	1.19 ± 0.35	381 ± 123
All types	20	185 ± 28	14	238 ± 61	1.67 ± 0.49	428 ± 83

Downloaded from http://mnras.oxfordjournals.org/ at Acquisitions on February 20, 2014

Astronomy Centre on behalf of the UK Particle Physics Research Council, the Netherlands Organization for Scientific Research and the Canadian National Research Council. The NASA/IPAC Extragalactic Data base (NED) is operated by the Jet Propulsion Laboratory, California Institute of Technology, under contract with the National Aeronautics and Space Administration. The Digitized Palomar Sky Survey was funded by the National Geographic Society and produced by the Space Science Telescope Institute from plates taken from the Oschin Schmidt Telescope. This is operated jointly by the California Institute of Technology and the Palomar Observatory.

REFERENCES

Anantharamaiah K. R., Viallefond F., Mohan N. R., Goss W. M., Zhao J. H., 2000, ApJ, 537, 613
Casoli F., Dickey J., Kazès I., Boselli A., Gavazzi G., Jore K., 1996, A&AS, 116, 193
Chini R., Krügel E., Lemke R., 1996, A&AS, 118, 47
Condon J. J., Helou G., Sanders D. B., Soifer B. T., 1993, AJ, 105, 1730
Dunne L., 2000, PhD thesis, University of Wales Cardiff
Dunne L., Eales S. A., 2001, MNRAS, 327, 697
Dunne L., Eales S., Edmunds M., Ivison R., Alexander P., Clements D. L., 2000, MNRAS, 315, 115
Elfhag T., Booth R. S., Höglund B., Johansson L. E. B., Sandqvist A., 1996, A&AS, 115, 439
Huchra J. P., Vogeley M. S., Geller M. J., 1999, ApJS, 121, 287
Kenney J. D., Young J. S., 1989, ApJ, 344, 171
Lavezzi T. E., Dickey J. M., 1998, AJ, 116, 2672
McDowell J. C. et al., 2003, ApJ, 591, 154
Maiolino R., Ruiz M., Rieke G. H., Papadopoulos P., 1997, ApJ, 485, 552
Sanders D. B., Mirabel I. F., 1985, ApJ, 298, L31
Sanders D. B., Scoville N. Z., Soifer B. T., 1991, ApJ, 370, 158
Sofue Y., Wakamatsu K., Taniguchi Y., Nakai N., 1993, PASJ, 45, 43
Soifer B. T., Neugebauer G., Matthews K., Becklin E. E., Ressler M., Werner M. W., Weinberger A. J., Egami E., 1999, ApJ, 513, 207
Theureau G., Bottinelli L., Coudreau-Durand N., Gouguenheim L., Hallet N., Loulergue M., Paturel G., Teerikorpi P., 1998, A&AS, 130, 333
Thomas H. C., Dunne L., Clemens M. S., Alexander P., Eales S., Green D. A., 2002, MNRAS, 329, 747 (Paper I)
Thomas H. C., Alexander P., Clemens M. S., Green D. A., Dunne L., Eales S., 2004, MNRAS, submitted (Paper III)
Tinney C. G., Scoville N. Z., Sanders D. B., Soifer B. T., 1990, ApJ, 362, 473
Wang Z., Kenney J. D., Ishizuki S., 1992, AJ, 104, 2097
Wiedner M. C., Wilson C. D., Harrison A., Hills R. E., Lay O. P., Carlstrom J. E., 2002, ApJ, 581, 229
Young J. S. et al., 1995, ApJS, 98, 219
Zhu M., Seaquist E. R., Davoust E., Frayer D. T., Bushouse H. A., 1999, AJ, 118, 145

APPENDIX A: D-ARRAY OBSERVATIONS

As noted above, a small sample of 13 of the larger (greater than 2.5 arcmin) SLUGS galaxies were observed with the VLA in D-array. These data were analysed in a similar way to the C-array data (see Section 2). Three of the galaxies observed (NGC 958, 5020 and 5962) were also observed in C-array, and the results for these galaxies are given above. Of the other galaxies observed, one (UGC 2369) was not detected in the D-array observations. The integrated H I images for the other nine galaxies are presented in Fig. A1.

Downloaded from http://mnras.oxfordjournals.org/ at Acquisitions on February 20, 2014

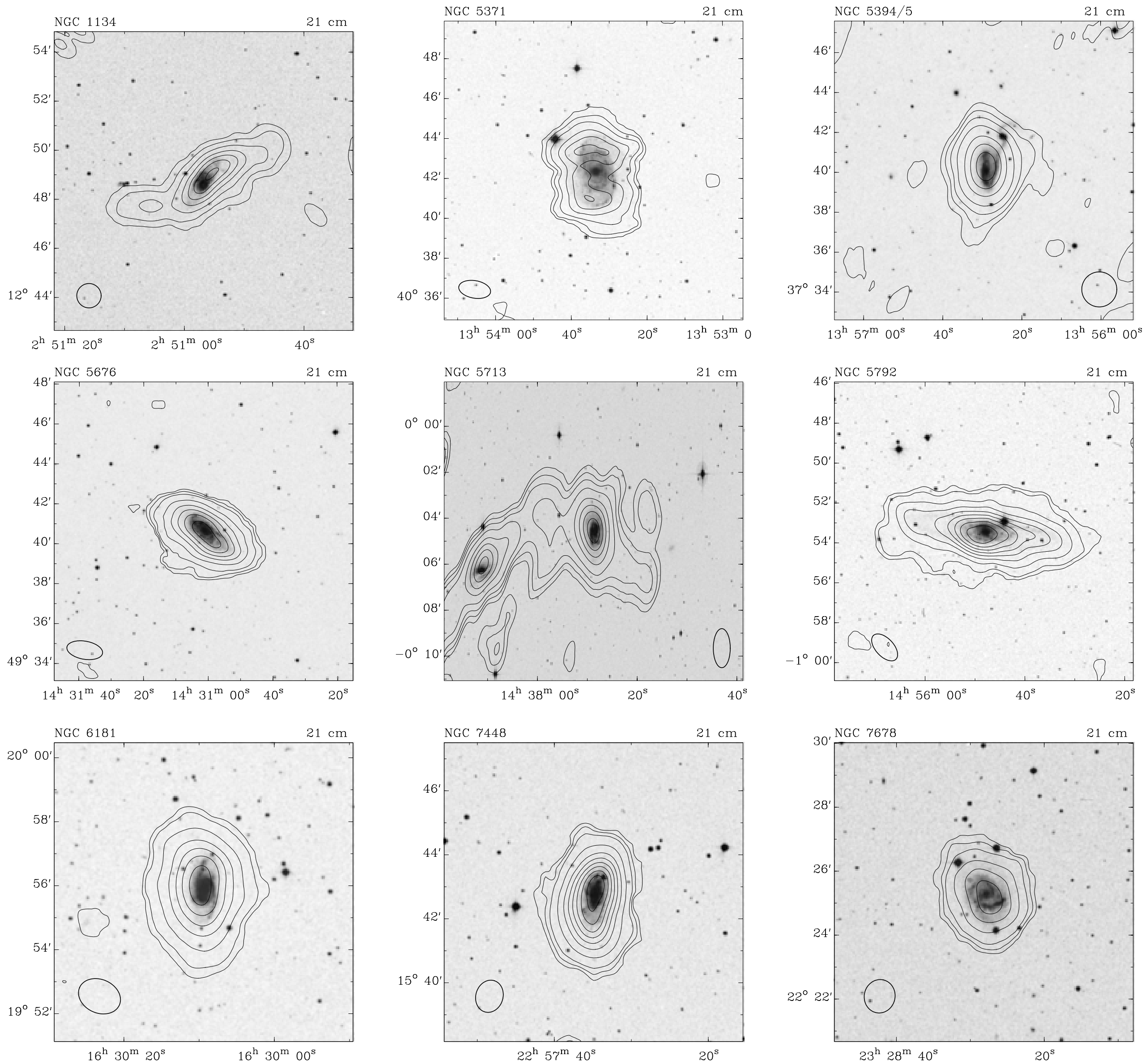

Figure A1. VLA H I images of galaxies observed in D-array. The contours are ± (0.5, 1, 3, 6, 9...) × 10^{20} atom cm^{-2}, and the resolution of each image is indicated by the ellipse in the bottom corner.

This paper has been typeset from a TEX/LATEX file prepared by the author.

Downloaded from http://mnras.oxfordjournals.org/ at Acquisitions on February 20, 2014